

# Shock manipulation in a Mach 2 free-jet inlet by thermal actuator

H. Yan\* \*\* and P.L. Zhang\*

\*Northwestern Polytechnical University

127 Youyi Xilu, Xi'an, Shaan xi Province, P.R.China 710072

\*\*Collaborative Innovation Center for Advanced Aero-Engine, Beijing, 100191, China

## Abstract

The mechanism of shock manipulation in a supersonic inlet using near-surface discharges is studied numerically. This inlet is comprised of two consecutive compression angles of 7 degree and 14 degree, and the design Mach number is 2. The near-surface discharge is modelled as a controllable equivalent heat source based on Joule heating effect of plasma. Results show that near-surface discharge can effectively improve the aerodynamic performance of the inlet at off-design condition by increasing total pressure recovery coefficient and reducing separation region. Once the thermal actuator is turned on, the boundary layer thickness is increased and an induced oblique shock is formed. It is found that the thickened boundary layer reshapes the original compression ramps and causes the intensity reduction of the two oblique shocks, leading to increase of the total pressure recovery coefficient. The effects of the input heat power and off-design incoming Mach number are studied. It is shown that two competing factors affect the overall aerodynamic performance of the inlet. One is the intensity of the induced shock, which increases with the input heat power and incoming Mach number, resulting in decrease of the total pressure recovery coefficient. The other one is the effective angles of compression corner, which decrease with the input heat power and incoming Mach number, resulting in increase of the total pressure recovery coefficient. Results show that the total pressure recovery coefficient increases first and then decreases with the input heat power. For different incoming Mach number is found the optimal input heat power range in which the total pressure recovery coefficient is higher than that without thermal actuator, and the flow capture ratio is 1.0.

## 1. Introduction

With advanced aircraft flying faster and higher, aircraft inlet needs to work in a more complex and broad flight condition. In order to make inlet work more stable and reliable, we can use flow control techniques to improve its aerodynamic performance by reducing the distortion of the flow field under off-design conditions. The near-surface electric discharge plasma as a flow control technique has been research focus in recent years. The main mechanism of glow discharge or quasi DC discharge plasma flow control without external magnetic field interference is mainly the Joule heating effect. When the gas between the electrodes of the plasma actuator is breakdown, gas temperature and pressure increase instantly, resulting in the increase of the boundary layer thickness. The displaced boundary layer acts like a virtual wedge, and induces oblique shocks, whose position and angle are strongly associated with features of plasma layer (temperature, pressure and density). One of the main features is related to the plasma heating gas due to recombination and V-T relaxation. Under ideal conditions, the vibration and decomposition of gas molecules absorb up to 90% of the total discharge energy temporarily, and then release in the downstream. The spatial and temporal behavior of the plasma instability shows high efficiency and low energy consumption in plasma control technique. Leonov et al. [1] at IVTAN of the Russian Academy of Science did experiment research on high speed air flow control by plasma discharge in 2002. They discussed the method to control the position and structure of oblique shock wave in the inlet by discharge [2]. Leonov et al. [3] continued their research and gave the experiment and numerical simulation results on the near-surface electric discharge plasma supersonic flow control, and the main purpose was to show the effect of the low temperature plasma on the structure of the supersonic flow and position of the shock wave on the compression ramp. Their results showed that when applying plasma aerodynamic actuation, the starting point of shock wave moved forward and its angle changed. Thus they verified the effectiveness of this method. Merriman et al. [4] at Ohio State University did experiments on changing the angle of shock wave by applying the spatial RF discharge plasma aerodynamic actuation. The experimental results showed that when the flow Mach number reached 2.5, the RF discharge caused the oblique shock change from 99 degree to 133 degree. At the same time, Palm et al. [5] studied the mechanism of changing the angle of shock wave by

applying plasma aerodynamic actuation. When using DC discharge whose heating effect was not strong, the angle of shock wave almost had no change. However when using RF discharge which had strong heating effect, the shock angle changed significantly. It proved the importance of thermal effect in plasma flow control.

The demand of improving aerodynamic performance and efficiency of high-speed aircrafts has increased since 2001, thus plasma flow control studies have showed a booming trend since then. In China, Air Force Engineering University, Chinese Aerodynamics Research and Development Center, BUAA, NWPU, Harbin Institute of Technology, National University of Defense Technology, Institute of Equipment and etc have done a lot of research work. Zhang and Li[6] did experimental and theoretical research about controlling the position and angle of the shock wave by using plasma actuation. In the Mach 2 supersonic wind tunnel, they used surface discharge to form plasma aerodynamic actuation. The experimental results showed that when plasma aerodynamic actuation applied, the shock moved forward and the shock angle was decreased. Yan[7] did simulations on the near-surface discharge shock wave control in the supersonic inlet inner wall whose design Mach number is 2. The results showed that in a certain range, the higher heat excitation energy was, the more distance the shock wave moved upstream. Cheng and Nie [8] at Institute of Equipment studied the influence of plasma thermal effect to supersonic flow structure. By numerical simulation, they studied the influence of quasi DC discharge or glow discharge plasma thermal effect on supersonic flow. The results showed that the length of plasma zone had little effect on control, but its thickness had great impact on control. When the plasma thickness increased, the shock angle increased, and the shock intersection point with the up wall moved upstream. It was also found when the Mach number increased, the intersection point moved downstream.

This paper further studies the effect of near-surface discharge on the shock structures in a supersonic free-jet inlet. The effect of the input heat power and incoming Mach number is considered. The total pressure recovery coefficient and flow capture ratio are used as criteria to determine the optimal input heat power range for different off-design Mach number.

## 2. Flow configuration and numerical model

### 2.1 Calculation conditions

According to the flight corridor, an air-breathing vehicle can fly at Mach number up to 5 at 15km. Therefore the design condition is a Mach 2 compression inlet with the freestream condition at the altitude of 15km, where the static temperatures and pressure are 200K,  $1.2 \times 10^4 Pa$  respectively. As shown in Figure 1 is a free-jet supersonic inlet model. From Figure 2, we can see that two oblique shocks are generated at two consecutive compression corners in the streamwise direction, and interact with each other impinging on the cowl lip. In a two-dimensional simulation, the surface discharge is modelled as a heat strip placed 20 mm upstream of the first compression corner. The heat strip is 10mm long in the streamwise direction and 3mm high in the wall-normal direction to emulate the volumetric effect of vibrational-translational (V-T) relaxation on gas heating.

The three-dimensional Navier-Stokes equations are solved by numerical discretization of space  $(x,y,z)$  and time  $(t)$ . The third-order accurate AUSM scheme is adopted for convective flux terms and the second order implicit method is used for time integration. The gradient reconstruction is based on node Green-Gauss method. Equations are solved using incomplete lower upper factorization (ILU, in conjunction with algebraic multi-grid method. The time step is fixed at  $1.5 \times 10^{-7} s$ , and the CFL number is 1. The SST turbulence model is used for the viscous assumption. The total pressure, total temperature and incoming Mach number are imposed at the inflow, upper and lower boundaries. The first-order extrapolation is used for the outflow. The wall is assumed as no-slip adiabatic condition. The Sutherland formula is used to compute the temperature-dependent viscosity coefficient. The relationship between  $C_p$  and temperature is based on fitting relationship proposed by Balakrishnan [9].

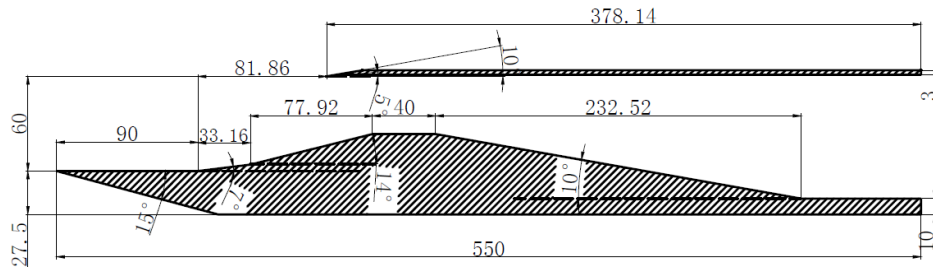


Figure 1: Mach 2 supersonic inlet model

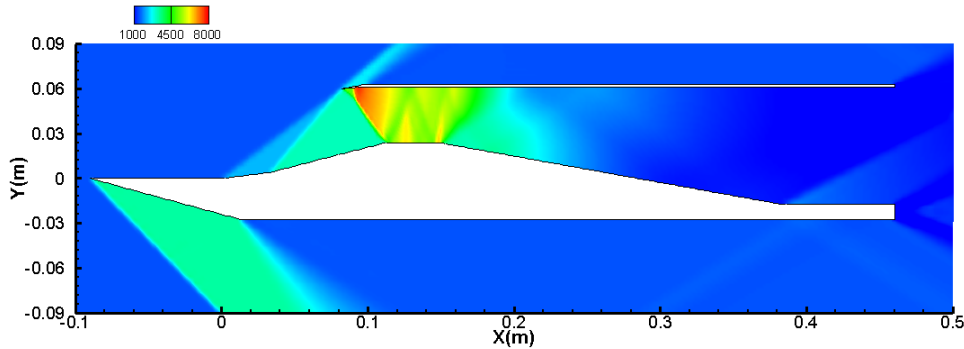


Figure 2: Pressure contours under Mach 2 design condition

## 2.2 Grid refinement

The computational domain is divided into three regions, as shown in Figure 3 in which the region B is the domain of interest. To ensure the accuracy of the calculation results and eliminate the effect of grid precision on calculation results, five different grids are used for the grid refinement study. The details are shown in Table 1. The incoming Mach number is fixed at the off-design condition of 2.5, and the heating power is set at 2kW.

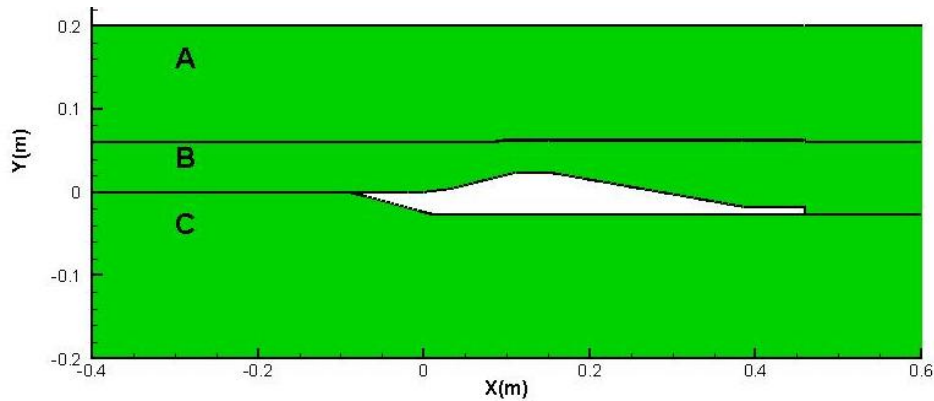


Figure 3: Computational domain and grid region

Table 1 Grid configuration

| Grid number | Minimum grid spacing                 | Stretching ratio | Number of grids in y direction |
|-------------|--------------------------------------|------------------|--------------------------------|
| 1           | $\Delta y = 0.24mm$ $\Delta x = 1mm$ | 1.08             | 58                             |
| 2           | $\Delta y = 0.12mm$ $\Delta x = 1mm$ | 1.04             | 116                            |

|   |                     |                    |      |     |
|---|---------------------|--------------------|------|-----|
| 3 | $\Delta y = 0.06mm$ | $\Delta x = 1mm$   | 1.02 | 232 |
| 4 | $\Delta y = 0.06mm$ | $\Delta x = 0.5mm$ | 1.02 | 232 |
| 5 | $\Delta y = 0.04mm$ | $\Delta x = 0.5mm$ | 1.02 | 280 |

Figure 4 shows the surface pressure profile in the x direction under five different grids. The predicted pressure for the coarsest grid (grid 1) is slightly lower than that for the other four grids, in which the predicted pressure is on top of each other. According to the requirement of the SST turbulence model,  $\Delta y^+$  is in the order of 1. Figure 5 shows the first grid spacing normal to the wall ( $\Delta y^+$ ) on the lower wall. All the five grids meet the requirement as shown in Figure 5. For the purpose of numerical accuracy and computational cost, the grid 3 is chosen for the following simulations.

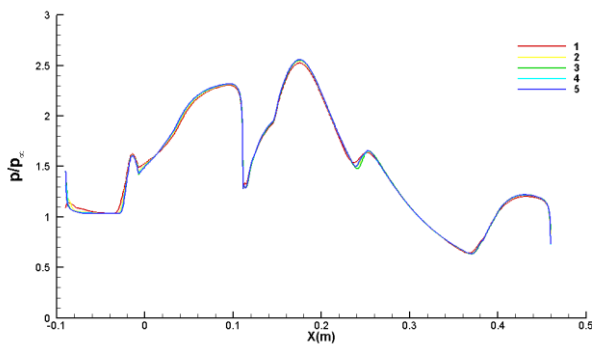


Figure 4: Surface pressure on the lower wall

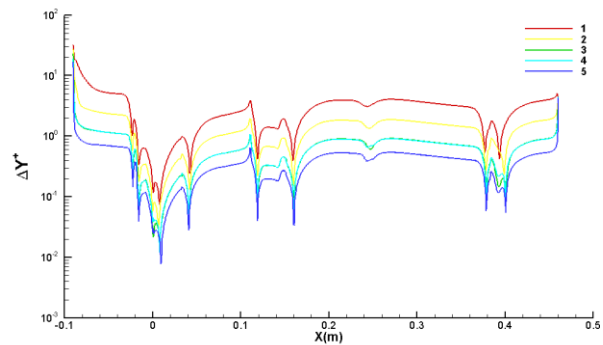
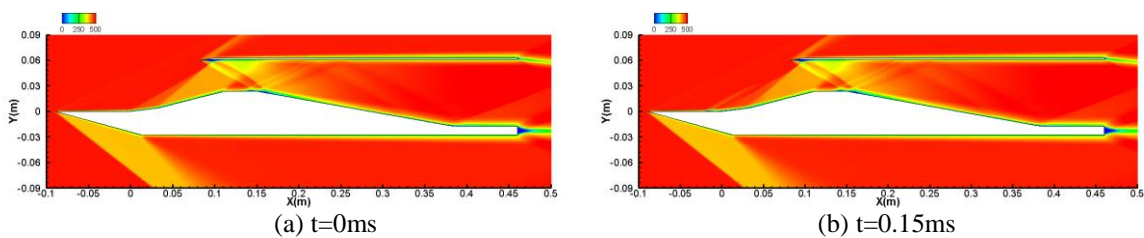


Figure 5: First grid on the lower wall

### 3. Numerical results and analysis

#### 3.1 Flow structures at off-design condition with thermal actuator

The unsteady flow structures are shown for Mach number of 2.5 and input heat power of 2kW. Figure 6 shows the instantaneous streamwise velocity contours during the first 0.75ms after the thermal actuator is turned on. Figure 6(a) shows the quasi-steady state without thermal actuator. It can be seen that the two original oblique shocks move into the inlet because the incoming Mach number is higher than the design Mach number. These two oblique shocks interact with the upper wall, leading to the separation of the boundary layer on the upper wall and larger total pressure loss. Once the thermal actuator is turned on, the boundary layer is heated and grows locally. A weak oblique shock starts to form as shown in Figure 6(b) due to sudden boundary layer displacement. At this input heat power, the induced shock intersects on the cowl lip. With time elapsing, the heating effect is extended downstream, and the boundary layer over the ramps is reshaped as shown in Figure 6(c)-6(f). The two sharp compression corners are smoothed out and become a gradually compressed surface, and two original oblique shocks are reduced to a series of compression waves which converge to one weak shock with a larger shock angle compared to the original ones. This weak shock wave moves upstream and impinges on the cowl lip as shown in Figure 6(f). It is obvious that the flow separation on the top wall is weakened by comparing Figure 6(a) and Figure 6(f).



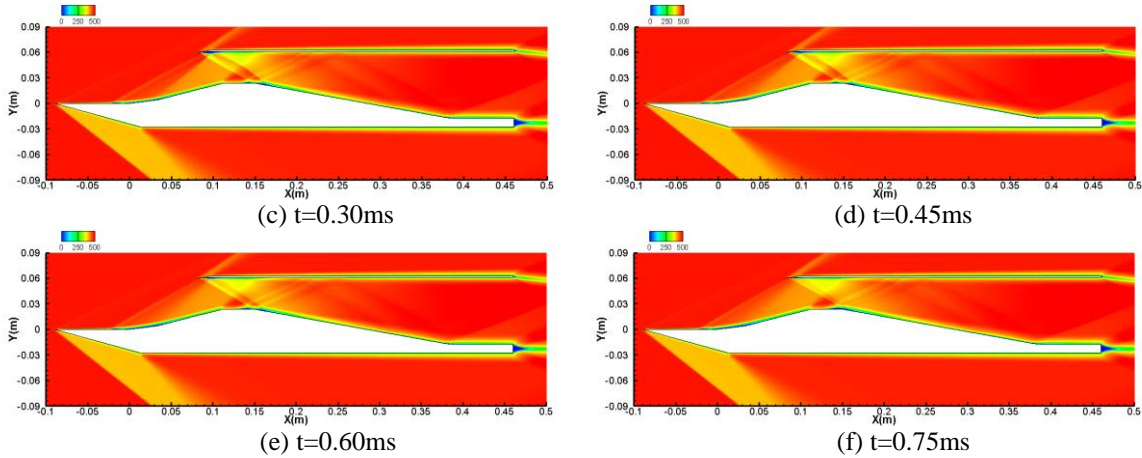


Figure 6: Instantaneous streamwise velocity contours

### 3.2 Effect of input heat power

The incoming Mach number is 2.5 and the input heat power is 1kW, 2kW, 3.5kW and 6.5kW. Figure 7 shows the streamwise velocity contours in the quasi-steady state for different input heat power. The boundary layer thickness grows with input heat power, which is demonstrated clearly by comparing the lower wall region in Figure 7(a) and 7(d), thus the induced shock intensity increases along with the increase of the shock angle. In Figure 7(b), the induced shock impinges right on the cowl lip for the input heat power of 2kW, while for other energy levels, the induced shock either intersects on the upper wall (Figure 7(a)), or moves upstream of the cowl lip (Figure 7(c) and (d)). The two original oblique shocks are weakened due to reshaping of the boundary layer to certain extent. The relative intensity of the induced shock and the weakened two oblique shocks is shown in the numerical Schlieren images in Figure 8. Two oblique shocks impinging on the upper wall are evident in Figure 8(a) when the thermal actuator is off. Once the thermal actuator is turned on, the induced shock comes into the picture with the two original shocks present at lower input heat power as shown in Figure 8(b). With increase of the input heat power, the two original shocks are weakened so significantly compared to the induced shock that they are not even present in Figure 8(c) and 8(d). Meanwhile, the induced shock is strengthened due to the local growth of the boundary layer at the fixed incoming Mach number, and the shock angle increases, resulting in decrease of the flow capture ratio.

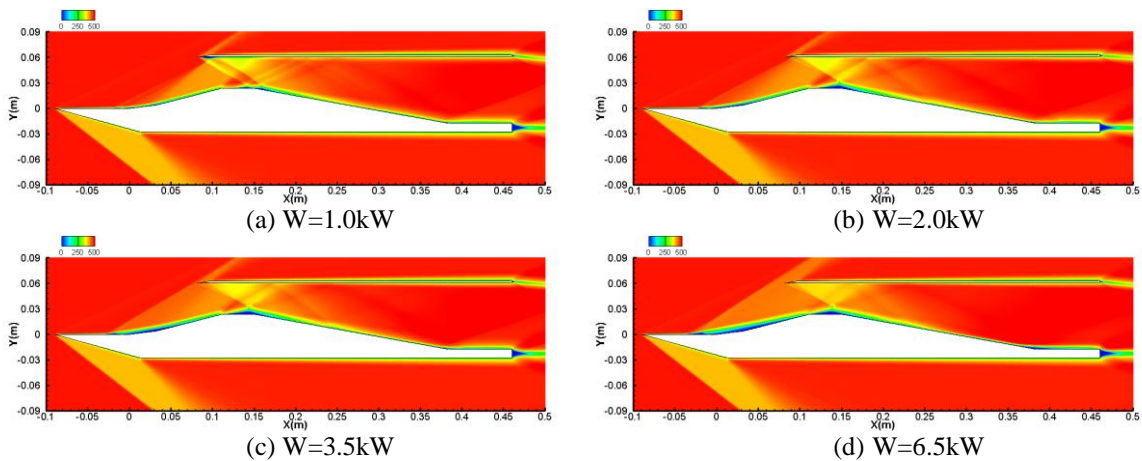
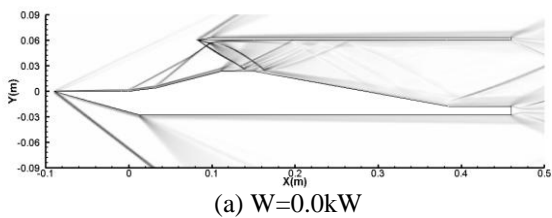


Figure 7: Streamwise velocity contours for incoming Mach number of 2.5



(a) W=0.0kW

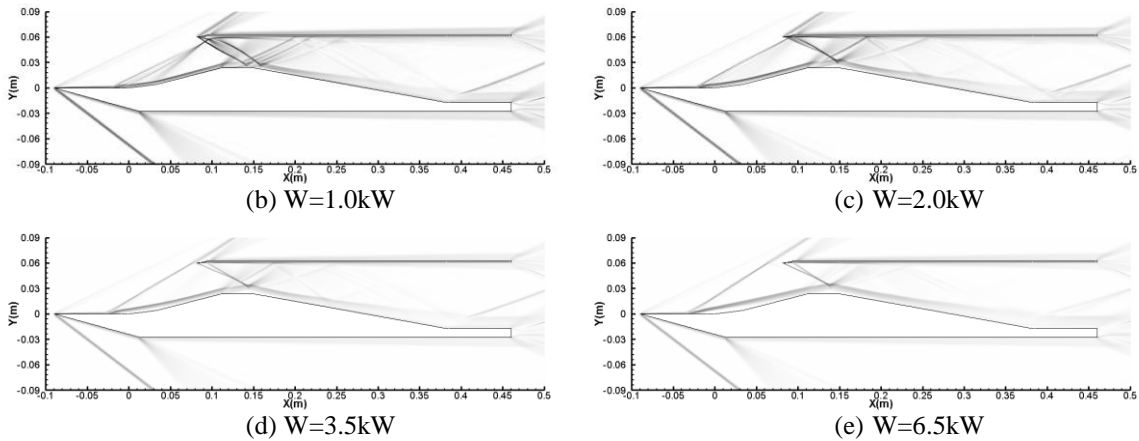


Figure 8: Numerical Schlieren images for incoming Mach number of 2.5

Figure 9 shows the surface pressure on the lower wall for different input heat power. It can be seen that the starting point of the induced oblique shock wave moves farther upstream with input heat power increasing and its strength increases as well. However, the two original oblique shocks are weakened with input heat power, which is consistent with the previous observation. For input heat power of 6.5kW, the induced shock is even stronger than the two original oblique shocks. It is also seen that the strength of the reflected shock wave on the upper wall decreases with input heat power. To evaluate the aerodynamic performance of inlet, the total pressure recovery coefficient is computed and shown in Table 2. It can be seen that adding thermal actuator does improve the total pressure recovery coefficient for low and median input energy level, but it does the opposite for high energy level. The reason for that is two folds. One is that with increase of the input energy the two original oblique shocks are weakened due to boundary layer reshaping, thus the total pressure recovery coefficient increases. On the other hand, with increase of the input energy the induced shock becomes stronger, resulting in decrease of the total pressure recovery coefficient. Once the later factor prevails, the total pressure recovery coefficient decreases. Therefore, for a fixed incoming Mach number, there will exist an optimal power range where the aerodynamic performance is improved. It will be discussed in the following section.

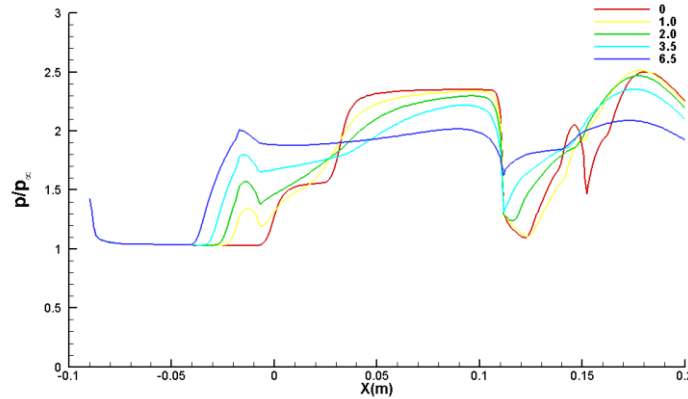


Figure 9: Surface pressure on the lower wall for incoming Mach number of 2.5

Table 2 Total pressure recovery coefficient for incoming Mach number of 2.5

| Input heat power (kW) | Total Pressure Recovery Coefficient |
|-----------------------|-------------------------------------|
| 0                     | 0.6108                              |
| 1                     | 0.6150                              |

|     |        |
|-----|--------|
| 2   | 0.6294 |
| 3.5 | 0.6224 |
| 6.5 | 0.5869 |

### 3.3 Effect of Mach number

The input heat power is fixed at 2kW and the incoming Mach number is 2.5, 3, 3.5 and 4. Figure 10 shows the streamwise velocity contours in the quasi-steady state for different Mach number. It can be seen that the boundary layer thickness increases with the incoming Mach number, and the boundary layer separation is more evident on the lower wall. The reason is that with increase of the incoming Mach number, the induced shock intensity increases, thus the adverse pressure gradient and temperature increase across the shock. This causes stronger shock/boundary layer interaction, and makes the boundary layer subject to more severe condition of separation. Table 3 shows the induced shock angle for different incoming Mach number. According to the supersonic theory, the induced shock angle is reduced with increase of the Mach number. However, because the boundary layer becomes thicker with Mach number increasing, this partially offsets the effect of the incoming Mach number on the induced shock angle. At the same time, the subsonic region in the near wall region becomes larger due to thickening of the boundary layer, which allows the disturbance propagating upstream, leading to the upstream movement of the shock starting point as shown in Figures 11 and 12. As discussed above, there are several competing factors working together to effect the shock structure in the supersonic inlet. In the current study, the shock impinging point on the upper wall is located at the same position for all the Mach number, which is clearly demonstrated in the numerical Schlieren images in Figure 13. The conclusion will be confirmed in the following section.

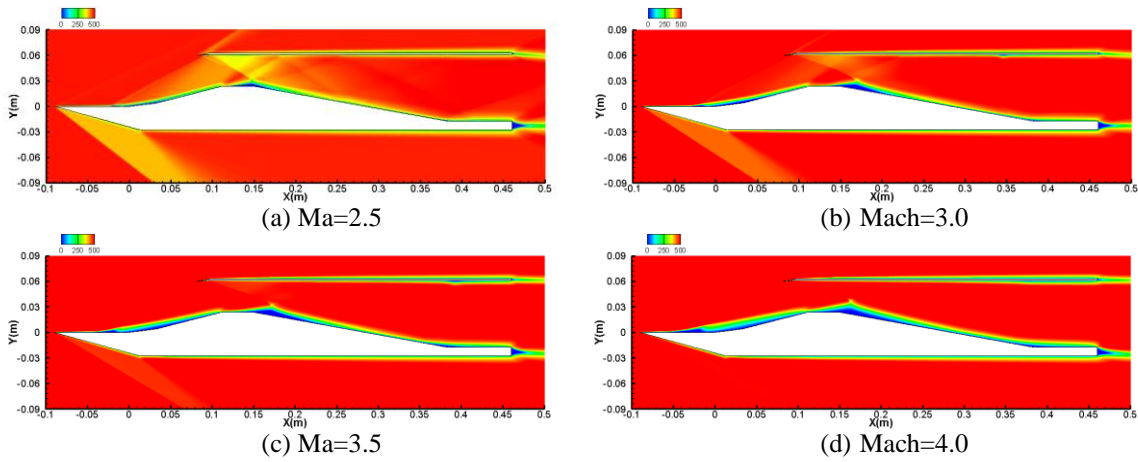


Figure 10: Streamwise velocity contours for input heat power of 2.0kW

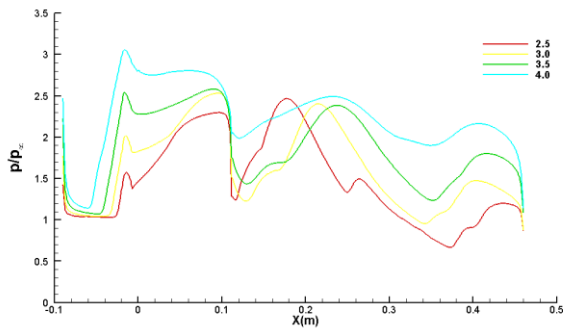


Figure 11: Surface pressure on the lower wall for input heat power of 2.0kW

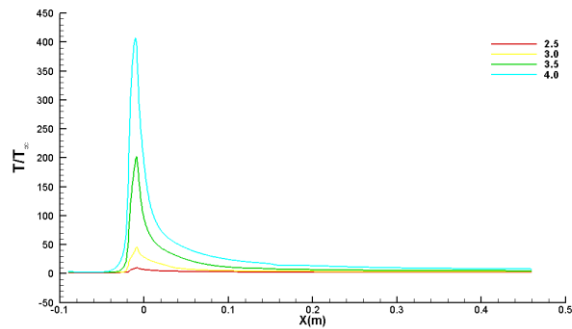


Figure 12: Temperature along the wall for input heat power of 2.0kW

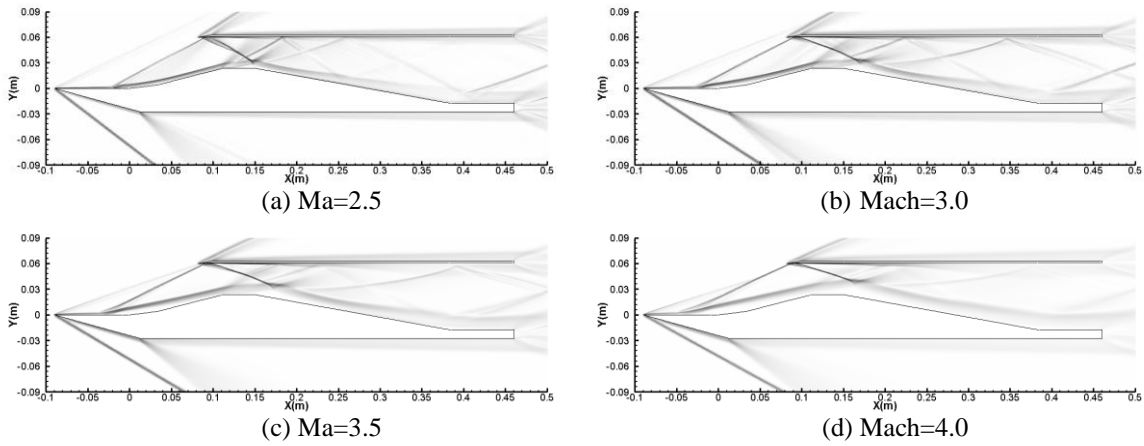


Figure 13: Numerical Schlieren image for input heat power of 2.0kW

Table 3 Induced shock angle for input heat power of 2.0kW

| Incoming Mach number | Shock angle |
|----------------------|-------------|
| 2.5                  | 30°         |
| 3.0                  | 28°         |
| 3.5                  | 26°         |
| 4.0                  | 23°         |

### 3.4 Optimal power range for different Mach numbers

From the above discussion, we can see that the use of thermal actuator can effectively improve the aerodynamic performance of the supersonic inlet which works under the off-design Mach number. However with increase of the input heat power, the total pressure recovery coefficient of the inlet shows a rise first followed by a decline, so there must exist an optimal power range corresponding to each Mach number. The Mach number considered in this section is 2.5, 3.0, 3.5 and 4.0. The total pressure recovery coefficient and flow capture ratio are used as two selection criteria. For Mach number of 2.5, the variation of total pressure recovery coefficient and flow capture ratio with the input heat power is shown in Table 4 and Figure 14(a). The total pressure recovery coefficient is increased, then decreased with the input heat power. The flow capture ratio is always 1.0 until the input heat power reaches 2.7kW, it starts to decrease. The reason is that at high input heat power the induced shock angle is large enough that the shock itself moves out of the inlet. The optimal power range of Mach number of 2.5 is 1.0kW-2.7kW in which the flow capture ratio remains at 1.0, while the total pressure recovery coefficient is higher than that without thermal actuator. Figures 14(b)-14(d) show the results for Mach number of 3.0, 3.5 and 4. Based on the above criterion, the optimal power range is 1.0kW-2.7kW for all the Mach number considered.

Table 4 Total pressure recovery coefficient and flow capture ratio for incoming Mach number of 2.5

| Input heat power (kW) | Total pressure recovery coefficient | Flow capture ratio |
|-----------------------|-------------------------------------|--------------------|
| 0.0                   | 0.6108                              | 1.0                |
| 1.0                   | 0.6150                              | 1.0                |

|     |        |        |
|-----|--------|--------|
| 1.3 | 0.6153 | 1.0    |
| 1.5 | 0.6227 | 1.0    |
| 1.7 | 0.6269 | 1.0    |
| 2.0 | 0.6294 | 1.0    |
| 2.3 | 0.6303 | 1.0    |
| 2.5 | 0.6311 | 1.0    |
| 2.7 | 0.6313 | 1.0    |
| 3.0 | 0.6289 | 0.9872 |
| 3.5 | 0.6224 | 0.9745 |
| 6.5 | 0.5869 | 0.9152 |
| 8.5 | 0.5660 | 0.8863 |

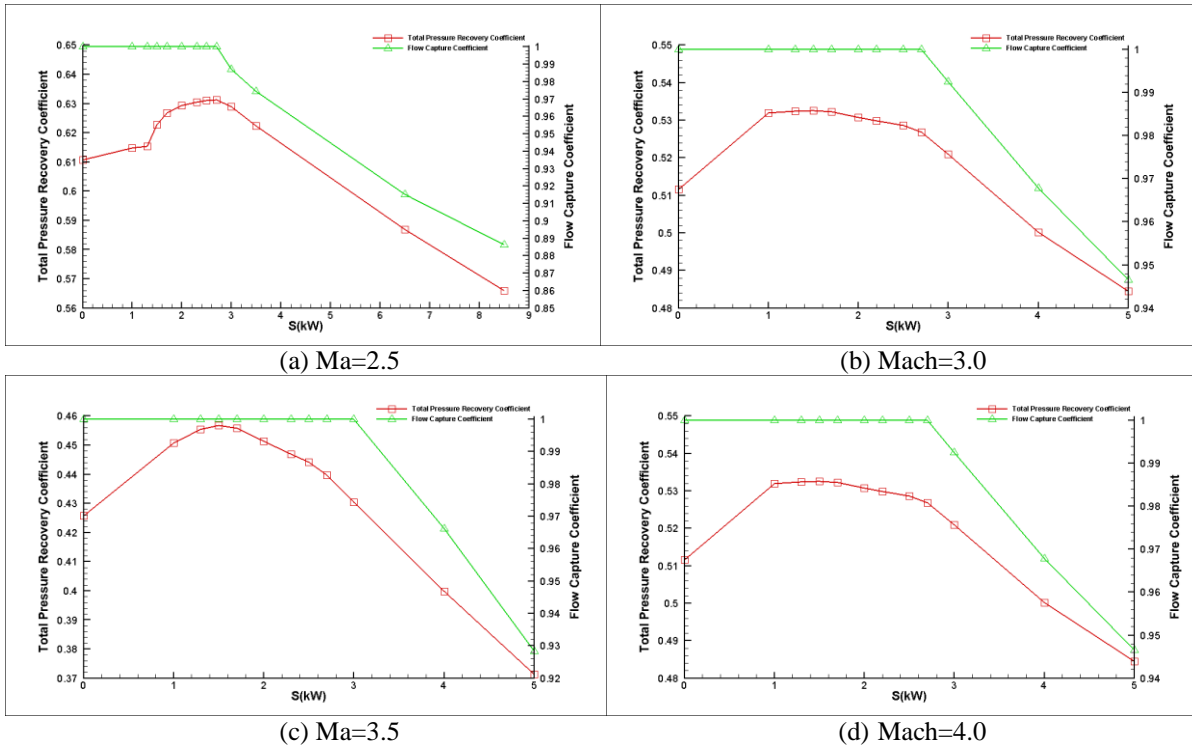


Figure 14: Total pressure recovery coefficient and flow capture ratio

#### 4. Conclusions

In this paper, the mechanism of near-surface discharge flow control in a free jet supersonic inlet is studied using numerical method. The effect of the input heat power and incoming Mach number on the shock structures is studied. Results show that the near-surface discharge plasma control can effectively improve the aerodynamic performance of the inlet under the off-design condition. The total pressure recovery coefficient is increased for the low and median heat power, while decreases for the high input heat power. The reason is analyzed. For the fixed incoming Mach number, with increase of the heat power the thickness of the boundary layer grows, so the original compression ramps are modified to a gradually compressed surface, leading to intensity attenuation of the two original oblique

shocks. On the other hand, the induced shock is strengthened with increase of the input heat power. Two factors are competing with each other at different heat power. For high heat power, the second factor dominates, so the total pressure recovery coefficient is decreased. While for low and median heat power, the first factor dominates, so the total pressure recovery coefficient is increased. The optimal power range for different incoming Mach number is found in terms of high total pressure recovery coefficient and flow capture ratio. For all the Mach number considered, the optimal input power range is 1.0kW-2.7kW.

## References

- [1] Leonov S. B., Bityurin V. and Savelkin K. The features of electro-discharge plasma control of high-speed gas flows. *AIAA Journal*, 2180, 2002.
- [2] Leonov S. B., Bityurin V. and Savelkin K. Progress in investigation for plasma control of duct-driven flows. *AIAA paper 2003-0699*, 2003.
- [3] Leonov S. B., Firsov A. A. and Yarantsev D. A. Flow control in model supersonic inlet by electrical discharge[R].*AIAA paper 2009-7367*, 2009.
- [4] Merriman S., Ploenjes E. and Palm P. Shock wave control by nonequilibrium plasmas in cold supersonic gas flows. *AIAA Journal*, 39(8): 1547-1552, 2001.
- [5] Palm P., Meyer R. and Plonjes E. Nonequilibrium Radio Frequency Discharge Plasma Effect on Conical Shock Wave:  $M = 2.5$  Flow. *AIAA Journal*, 41(3): 465-469, 2003.
- [6] Zhang B. L. and Li, Y. Research status of the plasma flow control to improve the aerodynamic performance of the propulsion system. *Aviation Maintenance and Engineering*, 4:63-65, 2010.
- [7] Yan H. Near-Surface Discharge in Supersonic Inlet Control. *AIAA paper 2013-0530*, 2013.
- [8] Cheng Y.F. and Nie, W.S. Influence of plasma thermal effect on the structure of supersonic flow field. *The Chinese Congress of Theoretical and Applied Mechanics*. 2011.
- [9] Balakrishnan A. Correlations for specific heats of air species to 50,000 K. *4th Joint Thermophysics and Heat Transfer Conference*. 1986,.